Obrabotka metallov (tekhnologiya, oborudovanie, instrumenty) = Metal Working and Material Science. 2023 vol. 25 no. 4 pp. 117–135
ISSN: 1994-6309 (print) / 2541-819X (online)
DOI: 10.17212/1994-6309-2023-25.4-117-135

NSTU NETI

Obrabotka metallov -
Metal Working and Material Science

Journal homepage: http://journals.nstu.ru/obrabotka_metallov

# Performance modeling and multi-objective optimization during turning AISI 304 stainless steel using coated and coated-microblasted tools

***Satish Chinchanikar** [a, *], **Mahendra Gadge** [b]*

Vishwakarma Institute of Information Technology, Survey No. 3/4, Kondhwa (Budruk), Pune - 411039, Maharashtra, India

[a] https://orcid.org/0000-0002-4175-3098, satish.chinchanikar@viit.ac.in; [b] https://orcid.org/0000-0002-8603-8653, Mahendra.gadge@viit.ac.in

ARTICLE INFO

*Article history*:
Received: 15 August 2023
Revised: 05 September 2023
Accepted: 09 September 2023
Available online: 15 December 2023

*Keywords*:
*AISI 304*
Cutting force
Tool life
Coated tools
Surface roughness
Multi-objective optimization

ABSTRACT

**Introduction.** High-speed machining of stainless steel has long been a focus of research. Due to characteristics such as low thermal conductivity and work hardening, *AISI 304* is considered to be a difficult material to cut. Machinability indicators provide important information about the efficiency and effectiveness of the machining process, enabling manufacturers to optimize their operations for increased productivity and precision. **The purpose of the work.** Coated carbide tools are most often used for machining *AISI 304* stainless steel. Few studies, meanwhile, have examined the effects of pre-and post-treated coated carbide tools when turning these alloys at high speeds. In addition, only a small number of studies have simultaneously optimized the cutting parameters while employing pre- and post-treated tools. **The methods of investigation.** The present work comparatively evaluates the performance of coated and coated-microblasted tools during the turning of *AISI 304* stainless steel. The tools were *PVD-AlTiN* coated, *PVD-AlTiN* coated with microblasting as a post-treatment (*coated-microblasted*), and *MTCVD-TiCN/*$Al_2O_3$ coated (*MTCVD*). The experimental-based mathematical models were developed to predict and optimize the turning performance. **Results and Discussion.** In this study, it is found that *PVD-AlTiN* coated tools have the lowest cutting forces and surface roughness, followed by *PVD-AlTiN* coated-microblasted and *MTCVD-TiCN/*$Al_2O_3$ coated tools. However, there is no significant difference observed in these responses for coated and coated-microblasted tools. It is found that the cutting forces increased with feed and depth of cut while decreasing with cutting speed. However, this effect is significant for *MTCVD*-coated tools. On the other hand, higher tool life is observed with *MTCVD-TiCN/*$Al_2O_3$ coated tools, followed by *PVD AlTiN* coated-microblasted and *PVD-AlTiN* coated tools. Tool life was largely affected by cutting speed. However, *PVD-AlTiN* coated tools exhibited this effect more noticeably. The models, with correlation coefficients found above 0.9, can be utilized to predict responses in turning *AISI 304* stainless steel. The optimization study revealed that turning *AISI 304* stainless steel with *MTCVD-TiCN/*$Al_2O_3$ coated tools incurs lower cutting forces of 18–27 N, produces a minimum surface roughness of 0.3–0.44 µm, and has a better tool life of 36–51 min compared to *PVD-AlTiN* coated (*C*) and *PVD-AlTiN* coated-microblasted (*CMB*) tools.

**For citation:** Chinchanikar S., Gadge M.G. Performance modeling and multi-objective optimization during turning AISI 304 stainless steel using coated and coated-microblasted tools. *Obrabotka metallov (tekhnologiya, oborudovanie, instrumenty) = Metal Working and Material Science*, 2023, vol. 25, no. 4, pp. 117–135. DOI: 10.17212/1994-6309-2023-25.4-117-135. (In Russian).

## Introduction

High-speed machining of stainless steel has long been a focus of research. Due to characteristics such as low thermal conductivity and tendency to work hardening, *AISI 304* steel is difficult to machine. One of the most stringent indicators of the efficiency and effectiveness of a machining process is tool life.

*He et al.* [1] revealed that the cutting temperature of a *TiN*-coated tool is lower than that of an uncoated one and increases with increasing cutting parameters. *Rao et al.* [2] multi-objectively optimized material removal rate and roughness during turning of SS 304. *Kulkarni et al.* [3] observed that cutting speed significantly affects the chip-tool interface temperature, and feed greatly affects the cutting forces during turning of *SS 304*. According to *Bouzid et al.* [4], when turning of *SS 304* with *Ti(C,N)/*$Al_2O_3$*/TiN* coated

*** Corresponding author**
*Chinchanikar Satish*, Ph.D. (Engineering), Professor
Vishwakarma Institute of Information Technology,
Pune - 411039, Maharashtra, India
**Tel.:** +91-2026950441, **e-mail:** satish.chinchanikar@viit.ac.in

tools, the cutting duration is the main factor influencing the flank wear, which was then followed by the cutting speed.

A study by *Sharma* and *Gupta* [5] showed that *TiAlN/TiN* coated carbide tools significantly reduced tool wear and roughness during turning of SS 304. *Patel et al.* [6] observed that mechanical properties and machining performance are influenced by the microstructure of cermet tools. *Dubovska et al.* [7] conducted a tool life study of carbide tools when turning of *AISI 304* austenitic stainless steel. *Sharma et al.* [8] carried turning of *AISI 304* steel using hybrid nanofluids with minimal lubrication. Their study developed models for forces and surface roughness. *Rao et al.* [9] optimized the surface roughness using the *Differential Evolution* (*DE*) algorithm in turning *SS 304*.

*Chen et al.* [10] turned *SS 304* using *CrWN* hard film tools. Their study optimized performance using *grey relational analysis* (*GRA*). *Patil et al.* [11] evaluated cryogenically treated and untreated carbide cutting tools for turning *AISI 304* steel. Lower surface roughness and tool wear was observed with cryogenically treated tools. In turning *SS 304*, *Singh et al.* [12] found that cutting speed was a dominant factor affecting surface roughness and depth of cut, and the cutting speed-feed rate interaction significantly affected flank wear.

*Lubis et al.* [13] obtained tool life data and analyzed the tool wear of coated tools in turning *AISI 304* stainless steel. *Khan et al.* [14] conducted a study on the impact of surface-treated and *AlCrN*-coated drills when drilling *SS 304* at different cutting speeds. *Bedi et al.* [15] observed better results when processing *SS 304* steel with rice bran oil than coconut oil. *Rathod et al.* [16] optimized turning of *SS 304* with coated carbide tools using the *Taguchi* and *TOPSIS* methods. *Sivaiah et al.* [17] analyzed the performance of micro-grooved tools during turning *AISI 304*. Textured tools performed better compared to untextured tools. *Moganapriya et al.* [18] found improved performance with *TiAlSiN* coated tools during machining of *SS 304*.

A group of researchers evaluated the chip-tool interface temperature during machining of *SS 304* [19–20]. Experimental findings showed a significant influence of cutting speed on the temperature generated during machining. *Patel et al.* [21] found that the tool life of *Ti*-based coated cermet tools is significantly influenced by the coating compositions. *Özbek et al.* [22] found that during *AISI 304* wet turning, the feed rate has a substantial impact on tool wear and surface roughness.

According to the analysis of the literature, coated tools have been mostly used by the researchers to machine *AISI 304* stainless steel. Few researchers, meanwhile, have examined the effects of pre-and post-treated coated carbide tools when turning these alloys at high speeds. In addition, only a small number of studies have simultaneously optimized the cutting parameters for improved machining performance while employing pre-and post-treated tools. In light of this, this study compares and contrasts the effectiveness of coated and coated-microblasted tools when turning *AISI 304* stainless steel. The machining capabilities of tools coated with single-layer *PVD AlTiN*, coated-microblasted, and multi-layer *MTCVD* $TiCN/Al_2O_3$ were assessed. To predict and improve turning performance, the experimentally validated models were developed.

## Experimental Design

Turning experiments were carried out on *AISI 304* stainless steel bar with a diameter and length of 70 and 500 mm, respectively. The material's composition is shown in table 1.

Fig. 1 depicts the high-precision CNC lathe used for the experiments. To investigate the machining performance under dry conditions, experiments were conducted using single-layer *PVD AlTiN* coated

Table 1

**Percentage composition of *AISI 304***

| *C* | *Si* | *Mn* | *P* | *S* | *Cr* | *Ni* | *N* | *Fe* |
|---|---|---|---|---|---|---|---|---|
| 0.033 | 0.88 | 1.98 | 0.037 | 0.013 | 18.37 | 8.82 | 0.11 | Balance |

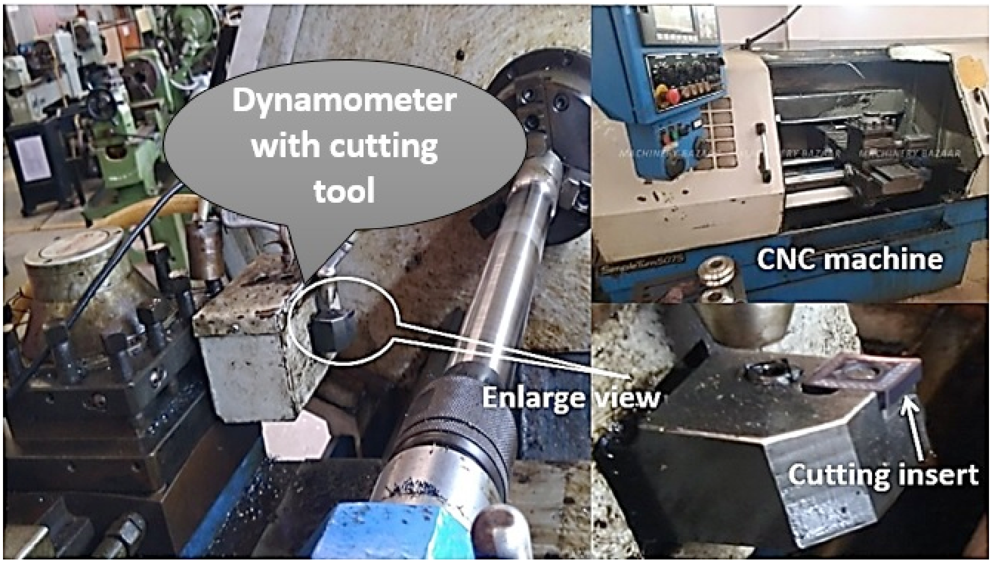


*Fig. 1.* Experimental set-up

(hereafter referred to as "*coated*"), single-layer *PVD AlTiN* coated and microblasted as a post-treatment (hereafter referred to as "*coated-microblasted*"), and multi-layer *MTCVD* $TiCN/Al_2O_3$ coated (hereafter referred to as "*MTCVD*"). At regular intervals along the length of the cut, flank wear was observed. Based on the results of the pilot tests, literature rewiev, and a manufacturer's recommendation, cutting parameters were selected.

Uncoated carbide inserts, marked in accordance with *ISO* as *CNMG120408MS*, are coated with aluminum titanium nitride (*AlTiN*) by physical vapor deposition (*PVD*) with pre- and post-treatment as described in table 1. The *CNMG120408* inserts, diamond-shaped with an 80° angle and 0.8 mm nose radius were rigidly mounted on a tool holder, marked in accordance with *ISO* as *PCBNR2525M12*, as shown in fig. 2.

The machining parameters were selected after a thorough literature study, catalog review, and searching experiments. Experimental matrix is shown in table 2. Flank wear was measured using a *Dino-Lite* digital microscope. Tool life ($T$) is obtained with flank wear of 0.2 mm. Longitudinal turning tests were carried out on a reliable, high-precision *CNC* lathe. A strain gauge-type lathe dynamometer was used to measure tangential force ($F_c$), feed force ($F_f$) and radial force ($F_r$) during the machining process. A *Taylor Hobson Surftronic* tester is used to evaluate surface roughness.

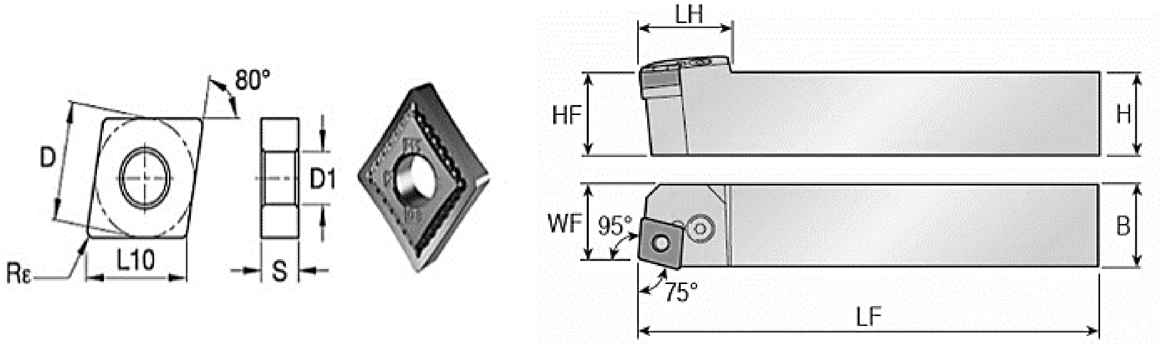


| | Insert particulars | | | | | Tool holder particulars | | | | | |
|---|---|---|---|---|---|---|---|---|---|---|---|
| Parameter | D | L10 | D1 | S | Rε | HF | H | B | LF | LH | WF |
| Dimension (mm) | 12.7 | 12.9 | 5.16 | 4.76 | 0.8 | 25 | 25 | 25 | 150 | 28 | 22.5 |

*Fig. 2.* Details of cutting insert and tool holder

Table 2

**Experimental matrix for *AISI 304* stainless steel**
**(*V*: Cutting speed, *f*: Feed, and *d*: Depth of cut)**

| Parameters | Expt. Run | | | | | | | | | | | | | | |
|---|---|---|---|---|---|---|---|---|---|---|---|---|---|---|---|
| | 1 | 2 | 3 | 4 | 5 | 6 | 7 | 8 | 9 | 10 | 11 | 12 | 13 | 14 | 15 |
| *V* (m/min) | 300 | 350 | 350 | 250 | 250 | 300 | 300 | 300 | 200 | 400 | 350 | 250 | 350 | 250 | 300 |
| *f* (mm/rev) | 0.1 | 0.08 | 0.12 | 0.08 | 0.12 | 0.05 | 0.1 | 0.15 | 0.1 | 0.1 | 0.08 | 0.12 | 0.12 | 0.08 | 0.1 |
| *D* (mm) | 0.5 | 0.4 | 0.4 | 0.4 | 0.4 | 0.3 | 0.3 | 0.3 | 0.3 | 0.3 | 0.2 | 0.2 | 0.2 | 0.2 | 0.1 |

## Results and Discussion

Turning experiments were performed on a *CNC* lathe using the cutting modes depicted in table 2. The surface roughness, three components of cutting force, namely, $F_c$, $F_f$, and $F_r$, and tool life (*T*) were measured until the flank wear reached 0.2 mm. Experimental results with different tools, namely *PVD-AlTiN* coated (*C*) tool, *PVD-AlTiN* coated-microblasted (*CMB*), and *MTCVD-TiCN/Al$_2$O$_3$* coated (*MTCVD*), are depicted in table 3.

### *Performance modeling*

Experimentally validated mathematical models were developed for the responses considered in this study for the various tools to better understand the turning characteristics. The regression equations were

Table 3

**Experimental results in turning *AISI 304* with different tools**

| Run no. | *PVD-AlTiN* coated (*C*) tool | | | | | *PVD-AlTiN* coated-microblasted (*CMB*) | | | | | *MTCVD-TiCN/Al$_2$O$_3$* coated (*MTCVD*) | | | | |
|---|---|---|---|---|---|---|---|---|---|---|---|---|---|---|---|
| | $F_c$ (N) | $F_f$ (N) | $F_r$ (N) | $R_a$ (μm) | *T* (min) | $F_c$ (N) | $F_f$ (N) | $F_r$ (N) | $R_a$ (μm) | *T* (min) | $F_c$ (N) | $F_f$ (N) | $F_r$ (N) | $R_a$ (μm) | *T* (min) |
| 1 | 108 | 44 | 17 | 0.93 | 8.1 | 118 | 48 | 21 | 0.88 | 9.81 | 111 | 55 | 26 | 1.14 | 18.4 |
| 2 | 69 | 27 | 15 | 0.62 | 10.3 | 69 | 33 | 16 | 0.57 | 11.2 | 78 | 38 | 21 | 0.69 | 14.4 |
| 3 | 98 | 41 | 16 | 0.68 | 7.6 | 98 | 43 | 21 | 0.74 | 6.8 | 118 | 53 | 26 | 0.85 | 9.3 |
| 4 | 78 | 31 | 16 | 0.72 | 14.4 | 88 | 36 | 17 | 0.77 | 16.4 | 98 | 40 | 22 | 0.85 | 21.3 |
| 5 | 88 | 51 | 18 | 0.87 | 11.2 | 137 | 51 | 23 | 0.96 | 11.1 | 137 | 56 | 27 | 1.05 | 14.3 |
| 6 | 59 | 22 | 13 | 0.47 | 18.1 | 49 | 18 | 12 | 0.45 | 19.5 | 49 | 22 | 17 | 0.55 | 24.6 |
| 7 | 69 | 33 | 14 | 0.65 | 12.6 | 69 | 35 | 18 | 0.65 | 13.9 | 88 | 40 | 24 | 0.74 | 18.8 |
| 8 | 88 | 47 | 17 | 0.83 | 10.4 | 98 | 46 | 26 | 0.81 | 10.3 | 121 | 59 | 34 | 0.97 | 14.6 |
| 9 | 78 | 34 | 16 | 0.96 | 15.1 | 88 | 38 | 20 | 0.93 | 15.9 | 98 | 45 | 26 | 0.99 | 22.1 |
| 10 | 59 | 29 | 15 | 0.42 | 6.8 | 69 | 33 | 18 | 0.50 | 7.2 | 78 | 40 | 23 | 0.62 | 9.4 |
| 11 | 48 | 19 | 11 | 0.39 | 14.8 | 39 | 22 | 14 | 0.42 | 16.4 | 39 | 29 | 21 | 0.47 | 18.6 |
| 12 | 61 | 33 | 14 | 0.66 | 15.3 | 59 | 40 | 19 | 0.70 | 16.3 | 78 | 40 | 27 | 0.72 | 20.8 |
| 13 | 56 | 31 | 13 | 0.51 | 10.6 | 59 | 33 | 18 | 0.52 | 11.8 | 59 | 45 | 26 | 0.65 | 15.7 |
| 14 | 54 | 23 | 12 | 0.57 | 17.6 | 39 | 28 | 14 | 0.61 | 21.8 | 49 | 28 | 22 | 0.62 | 26.6 |
| 15 | 39 | 17 | 10 | 0.37 | 16.4 | 29 | 24 | 13 | 0.40 | 17.4 | 29 | 23 | 21 | 0.46 | 22.6 |

created and its coefficient values were calculated using *DataFit* software. The developed mathematical models are shown in tables 4, 5, and 6 for *PVD-AlTiN* coated (*C*) tools, *PVD-AlTiN* coated-microblasted (*CMB*) tools, and *MTCVD-TiCN/*$Al_2O_3$ coated (*MTCVD*) tools, respectively.

The developed models have *R*-squared values closer to 0.95, indicating its reliability in predicting responses based on the variation proportion in the data points during turning of SS 304 when using *PVD-AlTiN* coated (*C*) tools (Eqs. 1 to 5), *PVD-AlTiN* coated-microblasted (*CMB*) tools (Eqs. 6 to 10), and *MTCVD-TiCN/*$Al_2O_3$ coated (*MTCVD*) tools (Eqs. 11 to 15).

Table 4

**Mathematical models for *PVD-AlTiN* coated (*C*) tool**

| Responses | Developed model | R-squared value | Eq. no. |
|---|---|---|---|
| Tangential force ($F_c$) | $= 1271.76V^{-0.195}f^{0.426}d^{0.652}$ | 0.92 | (1) |
| Feed force ($F_f$) | $= 3218.41V^{-0.321}f^{0.913}d^{0.547}$ | 0.95 | (2) |
| Radial force ($F_r$) | $= 121.93V^{-0.192}f^{0.263}d^{0.350}$ | 0.91 | (3) |
| Surface roughness ($R_a$) | $= 620.52V^{-0.902}f^{0.482}d^{0.513}$ | 0.93 | (4) |
| Tool life ($T$) | $= 231.25V^{-0.853}f^{-0.618}d^{-0.371}$ | 0.91 | (5) |

Table 5

**Mathematical models for *PVD-AlTiN* coated-microblasted (*CMB*) tool**

| Responses | Developed model | R-squared value | Eq. no. |
|---|---|---|---|
| Tangential force ($F_c$) | $= 38002.71V^{-0.559}f^{0.821}d^{0.980}$ | 0.96 | (6) |
| Feed force ($F_f$) | $= 2445.18V^{-0.333}f^{0.786}d^{0.432}$ | 0.95 | (7) |
| Radial force ($F_r$) | $= 369.13V^{-0.171}f^{0.739}d^{0.272}$ | 0.97 | (8) |
| Surface roughness ($R_a$) | $= 543.49V^{-0.866}f^{0.524}d^{0.470}$ | 0.98 | (9) |
| Tool life ($T$) | $= 141.73V^{-0.754}f^{-0.647}d^{-0.348}$ | 0.92 | (10) |

Table 6

**Mathematical models for *MTCVD-TiCN/*$Al_2O_3$ coated (*MTCVD*) tool**

| Responses | Developed model | R-squared value | Eq. no. |
|---|---|---|---|
| Tangential force ($F_c$) | $= 29772.68V^{-0.485}f^{0.932}d^{0.819}$ | 0.96 | (11) |
| Feed force ($F_f$) | $= 927.66V^{-0.093}f^{0.874}d^{0.463}$ | 0.97 | (12) |
| Radial force ($F_r$) | $= 250.89V^{-0.142}f^{0.618}d^{0.079}$ | 0.92 | (13) |
| Surface roughness ($R_a$) | $= 153.75V^{-0.602}f^{0.523}d^{0.554}$ | 0.95 | (14) |
| Tool life ($T$) | $= 551.62V^{-0.917}f^{-0.579}d^{-0.324}$ | 0.91 | (15) |

Further, for a better understanding, cutting forces (figs. 3–5), surface roughness (fig. 6), and tool life (fig. 7) are plotted using the developed models varying with cutting parameters for coated (*C*), coated-microblasted (*CMB*), and *MTCVD* tools. Fig. 3, *a* depicts tangential cutting forces for coated (*C*), coated-microblasted (*CMB*), and *MTCVD* tools varying with cutting speed at $f$ = 0.1 mm/rev and $d$ = 0.3 mm, respectively. The cutting forces can be seen as decreasing with the cutting speed. It could be attributed to an increase in the cutting speed increases the cutting temperature making the material soft and lowering the cutting force. Lower cutting forces can be seen for *PVD-AlTiN* coated (*C*) tools and higher forces for *MTCVD-TiCN/*$Al_2O_3$ coated (*MTCVD*) tools. However, no prominent difference in the tangential cutting force can be seen for the different tools.

Fig. 3, *b* displays the tangential cutting forces that vary with feed for coated (*C*), coated-microblasted (*CMB*), and *MTCVD* tools at $V$ = 300 m/min and $d$ = 0.3 mm.

And fig. 3, *c* depicts tangential cutting forces for coated (*C*), coated-microblasted (*CMB*), and *MTCVD* tools varying with depth of cut at $V$ = 300 m/min and $f$ = 0.1 mm/rev, respectively.

Cutting forces increase with feed and depth of cut, and the effect is more pronounced for *MTCVD-TiCN/*$Al_2O_3$ coated tools than for *PVD-AlTiN* coated tools (*C*) and *PVD-AlTiN* coated microblasted (*CMB*) tools. The lower cutting forces using *PVD-AlTiN* coated tools (*C*) and *PVD-AlTiN* coated microblasted (*CMB*) tools can be explained by the lower coefficient of friction and sharper edge radius of the single-layer *PVD-AlTiN* coated tool compared to multilayer *MTCVD-TiCN/*$Al_2O_3$ coated (*MTCVD*) tools. The phenomenon of lower friction for *PVD-AlTiN* coated tools results in lower cutting force compared to *MTCVD-TiCN/*$Al_2O_3$ coated tools.

Fig. 4, *a* and fig. 5, *a* depict feed and radial forces, respectively, for coated (*C*), coated-microblasted (*CMB*), and *MTCVD* tools, varying with cutting speed at $f$ = 0.1 mm/rev and $d$ = 0.3 mm, respectively. Fig. 4, *b* and fig. 5, *b* show the dependence of the feed force and radial force on the feed value at $V$ = 300 m/min and $d$ = 0.3 mm, respectively. Fig. 4, *c* and fig. 5, *c* depict feed and radial forces, respectively, for coated (*C*), coated-microblasted (*CMB*), and *MTCVD* tools, varying with depth of cut at $V$ = 300 m/min and

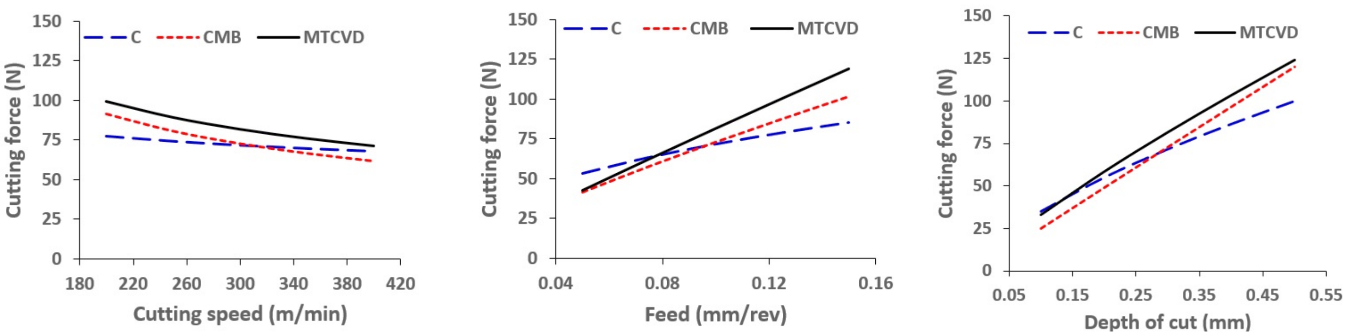


*a* *b* *c*

*Fig. 3.* Tangential force ($F_c$) for different tools varying with (*a*) $V$, (*b*) $f$, and (*c*) $d$

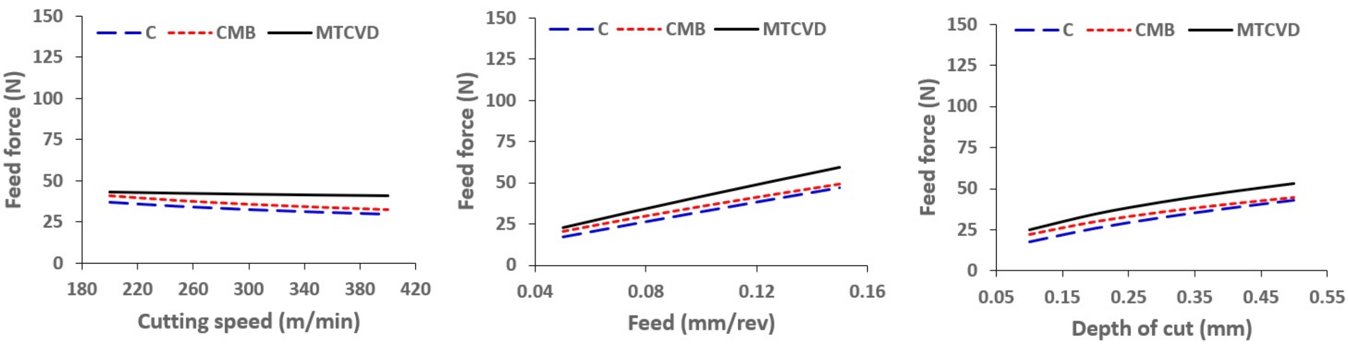


*a* *b* *c*

*Fig. 4.* Feed force ($F_f$) for different tools varying with (*a*) $V$, (*b*) $f$, and (*c*) $d$

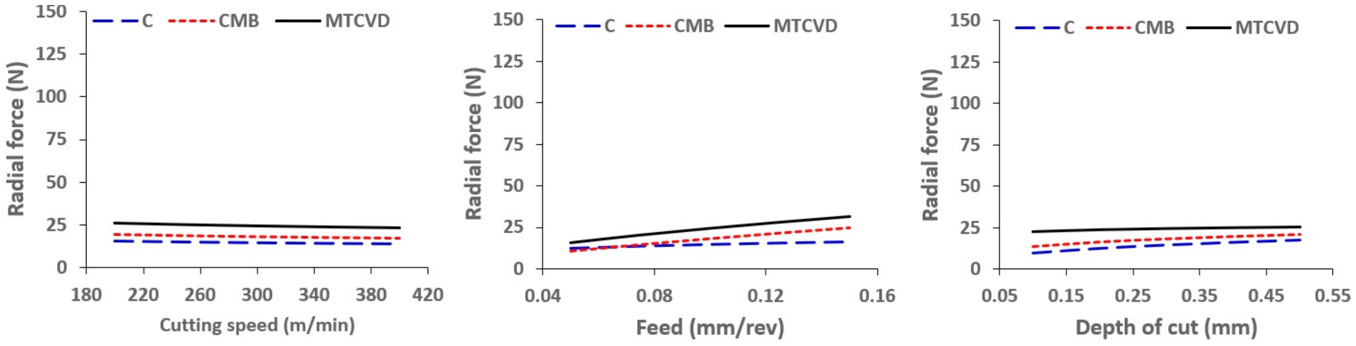


*a* *b* *c*

*Fig. 5.* Radial force ($F_r$) varying with (*a*) *V*, (*b*) *f*, and (*c*) *d*

*f* = 0.1 mm/rev, respectively. The feed forces can be noticed as increasing with the feed and depth of cut and being negligibly affected by the cutting speed. Lower feed forces are observed for *PVD-AlTiN* coated (*C*) tools and higher forces are observed for *MTCVD-TiCN/*$Al_2O_3$ coated (*MTCVD*) tools. However, no prominent difference in the feed force can be noticed for coated and coated-microblasted tools. The radial forces can be noticed as negligibly affected by the cutting parameters. Higher radial forces can be seen for *MTCVD-TiCN/*$Al_2O_3$ coated (*MTCVD*) tools.

Figs. 6 and 7 depict surface roughness and tool life, respectively, for coated (*C*), coated-microblasted (*CMB*), and *MTCVD* tools, varying with *V* = 300 m/min, *f* = 0.1 mm/rev, and *d* = 0.3 mm, respectively. It can be seen that the surface roughness decreases with increasing *V* (fig. 6, *a*) and increases with increasing *f* (fig. 6, *b*) and *d* (fig. 6, *c*). Lower surface roughness can be seen for *PVD-AlTiN* coated (*C*) tools and higher surface roughness for *MTCVD-TiCN/*$Al_2O_3$ coated (*MTCVD*) tools. Surface roughness is significantly affected by feed, especially for *MTCVD*-coated tools. However, there is no significant difference between coated tools and microblasted tools.

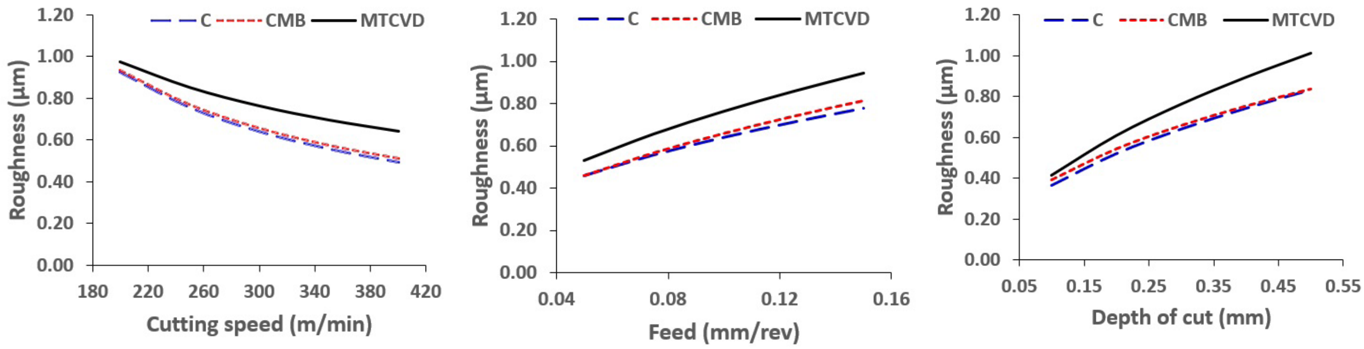


*a* *b* *c*

*Fig. 6.* Surface roughness ($R_a$) varying with (*a*) *V*, (*b*) *f*, and (*c*) *d*

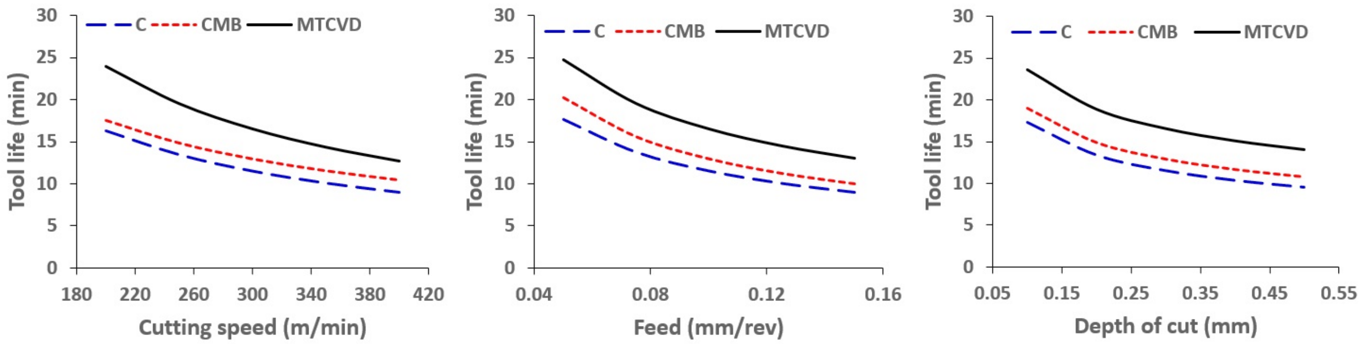


*a* *b* *c*

*Fig. 7.* Tool life (*T*) varying with (*a*) *V*, (*b*) *f*, and (*c*) *d*

When changing parameters, one may observe a decrease in tool life parameters. Cutting speed can be considered as having the greatest impact on tool life, followed by feed and depth of cut. The highest tool life can be seen for *MTCVD* tools, followed by coated-microblasted and coated tools. This can be attributed to the thicker coating with an average thickness of 22 μm compared to the thinner coating with an average thickness of 3 μm. Further, the $Al_2O_3$ coating layer assisted to increase tool life by forming a protective aluminum oxide layer on the coated tool during machining, which has protected the tool from oxidation and the loss of cutting elements from the tool. Further, the *TiCN* layer of the coating provided higher adhesion between the coating and the substrate.

### *Multi-objective optimization*

Researchers have made several attempts to optimize turning process parameters. However, limited studies optimized the turning of *AISI 304* using coated, coated-microblasted, and *MTCVD* tools. The study uses a *desirability function* technique to optimize turning parameters to achieve minimal cutting forces, surface roughness, and maximum tool life. Using Eq. 16, each response variable ($R_i$) is converted into a desirability function ($D_i$), and Eq. 17 transforms the optimization of multiple response variables into the optimization of a single desirability function ($D_M$). The process variables and a variety of possible response functions are shown in table 7.

$$D_i = \begin{Bmatrix} 0,1 \text{ if } R_i \le R_{\min} \\ \dfrac{R_i - R_{\min}}{R_{\max} - R_{\min}} \text{ if } R_{\min} \le R_i \le R_{\max} \\ 1,0 \text{ if } R_i \ge R_{\max} \end{Bmatrix}; \quad (16)$$

$$D_M = \left(D_1 \times D_2 \times D_3 \times - - - \times D_n\right)^{1/n}. \quad (17)$$

The one-sided transformation is used to transform each response *Ri* into its corresponding *Di* [23, 24]. By substituting all conceivable combinations and permutations of cutting parameters (around 10,000 data

Table 7

**Process variables and the range of response functions**

| Process variables and responses | Goal | *PVD-AlTiN* coated (*C*) tool | | *PVD-AlTiN* coated-microblasted (*CMB*) | | *MTCVD-TiCN/Al$_2$O$_3$* coated (*MTCVD*) | |
|---|---|---|---|---|---|---|---|
| | | Min. limit | Max. limit | Min. limit | Max. limit | Min. limit | Max. limit |
| Cutting speed (*V*) (m/min) | Is in range | 200 | 400 | 200 | 400 | 200 | 400 |
| Feed (*f*) (mm/rev) | Is in range | 0.05 | 0.15 | 0.05 | 0.15 | 0.05 | 0.15 |
| Depth of cut (*d*) (mm) | Is in range | 0.1 | 0.5 | 0.1 | 0.5 | 0.1 | 0.5 |
| Tangential cutting force ($F_c$) (N) | Minimize | 24.5 | 128.3 | 11.9 | 209.9 | 15.1 | 220.4 |
| Feed force ($F_f$) (N) | Minimize | 8.7 | 71.1 | 11.7 | 69.9 | 13.3 | 78.3 |
| Radial force ($F_r$) (N) | Minimize | 7.8 | 21 | 7.7 | 30.4 | 14 | 34.6 |
| Surface roughness ($R_a$) (μ*m*) | Minimize | 0.20 | 1.46 | 0.21 | 1.47 | 0.24 | 1.59 |
| Tool life (*T*) (min) | Maximize | 5.82 | 37.7 | 6.7 | 40.3 | 8.5 | 51.1 |

points) in the developed mathematical models that fall within the parameters chosen in the current study, minimum and maximum limits of response functions are obtained. One-sided transformation for different responses for *PVD-AlTiN* coated (*C*), *PVD-AlTiN* coated-microblasted (*CMB*), and *MTCVD-TiCN/*$Al_2O_3$ (*MTCVD*) tools can be represented considering the lower and higher limits of the respective responses.

One-sided transformation for different responses for *PVD-AlTiN* coated (*C*) tools (Eqs. 18–22), *PVD-AlTiN* coated-microblasted (*CMB*) tools (Eqs. 23–27), and *MTCVD-TiCN/*$Al_2O_3$ coated tools (*MTCVD*) (Eqs. 28–32) are given in tables 8, 9, 10, respectively.

For each level of independent parameters, $DF_c$, $DF_f$, $DF_r$, $Dr_a$ and $D_T$ were calculated using Eqs. 18–22 for *PVD-AlTiN* coated tools, Eqs. 23–27 for *PVD-AlTiN* coated-microblasted tools, and Eqs. 28–32 for *MTCVD-TiCN/*$Al_2O_3$ coated tools. Then, a single desirability function, $D_M$ was calculated by substituting $DF_c$, $DF_f$, $DF_r$, $Dr_a$ and $D_T$ in Eq. 17. The optimal parameter was chosen based on the solution with the highest desirability ($D_M$).

In the present study a family of optimal solutions having single desirability function ($D_M$) of above 0.9 are selected and are shown in tables 11, 12, and 13 for *PVD-AlTiN* coated (*C*) tools, *PVD-AlTiN* coated-microblasted (*CMB*) tools, and *MTCVD-TiCN/*$Al_2O_3$ coated tools, respectively.

In the present study, $V$ = 200–290 m/min, $f$ = 0.05–0.055 mm/rev, and $d$ = 0.1–0.12 mm were found to be the optimal parameters when using *PVD-AlTiN* coated (*C*) tools and *MTCVD-TiCN/*$Al_2O_3$ coated tools. However, $V$ = 200–320 m/min, $f$ = 0.05–0.055 mm/rev and $d$ = 0.1–0.12 mm, are the optimal cutting condition when using *PVD-AlTiN* coated-microblasted (*CMB*) tools. The optimization study reveals that in comparison with *C*-coated and *CMB*-coated tools, when turning *AISI 304* stainless steel with *MTCVD* coated tools, the cutting forces are significantly less and amount to 18–27 N, and the minimum surface roughness reaches 0.3–0.44 µm, while the tool life increases to 36–51 min.

Table 8

**One-sided transformation for *PVD-AlTiN* coated (*C*) tools**

| Desirability for tangential cutting force ($DF_c$) (Eq. 18) | Desirability for feed force ($DF_f$) (Eq. 19) |
|---|---|
| $DF_c = \begin{cases} 0, & F_c \geq 128.3 \\ \dfrac{F_{c_{\max}} - F_{c_i}}{F_{c_{\max}} - F_{c_{\min}}}, & F_{c_{\min}} \leq F_{c_i} \leq F_{c_{\max}} \\ 1, & F_c \leq 24.5 \end{cases}$ | $DF_f = \begin{cases} 0, & F_f \geq 71.1 \\ \dfrac{F_{f_{\max}} - F_{f_i}}{F_{f_{\max}} - F_{f_{\min}}}, & F_{f_{\min}} \leq F_{f_i} \leq F_{f_{\max}} \\ 1, & F_f \leq 8.7 \end{cases}$ |
| Desirability for radial force ($DF_r$) (Eq. 20) | Desirability for surface roughness ($DR_a$) (Eq. 21) |
| $DF_r = \begin{cases} 0, & F_r \geq 21 \\ \dfrac{F_{r_{\max}} - F_{r_i}}{F_{r_{\max}} - F_{r_{\min}}}, & F_{r_{\min}} \leq F_{r_i} \leq F_{r_{\max}} \\ 1, & F_r \leq 7.8 \end{cases}$ | $DR_a = \begin{cases} 0, & R_a \geq 1.46 \\ \dfrac{R_{a_{\max}} - R_{a_i}}{R_{a_{\max}} - R_{a_{\min}}}, & R_{a_{\min}} \leq R_{a_i} \leq R_{a_{\max}} \\ 1, & R_a \leq 0.2 \end{cases}$ |
| Desirability for tool life ($D_T$) (Eq. 22) | |
| $D_T = \begin{cases} 0, & T \leq 5.82 \\ \dfrac{T_i - T_{\min}}{T_{\max} - T_{\min}}, & T_{\min} \leq T_i \leq T_{\max} \\ 1, & T \geq 37.7 \end{cases}$ | |

Table 9

**One-sided transformation for *PVD-AlTiN* coated-microblasted (*CMB*) tools**

| Desirability for tangential cutting force ($DF_c$) (Eq. 23) | Desirability for feed force ($DF_f$) (Eq. 24) |
|---|---|
| $DF_c = \begin{cases} 0, & F_c \ge 209.9 \\ \dfrac{F_{c_{\max}} - F_{c_i}}{F_{c_{\max}} - F_{c_{\min}}}, & F_{c_{\min}} \le F_{c_i} \le F_{c_{\max}} \\ 1, & F_c \le 11.9 \end{cases}$ | $DF_f = \begin{cases} 0, & F_f \ge 69.9 \\ \dfrac{F_{f_{\max}} - F_{f_i}}{F_{f_{\max}} - F_{f_{\min}}}, & F_{f_{\min}} \le F_{f_i} \le F_{f_{\max}} \\ 1, & F_f \le 11.7 \end{cases}$ |
| Desirability for radial force ($DF_r$) (Eq. 25) | Desirability for surface roughness ($DR_a$) (Eq. 26) |
| $DF_r = \begin{cases} 0, & F_r \ge 30.4 \\ \dfrac{F_{r_{\max}} - F_{r_i}}{F_{r_{\max}} - F_{r_{\min}}}, & F_{r_{\min}} \le F_{r_i} \le F_{r_{\max}} \\ 1, & F_r \le 7.7 \end{cases}$ | $DR_a = \begin{cases} 0, & R_a \ge 1.47 \\ \dfrac{R_{a_{\max}} - R_{a_i}}{R_{a_{\max}} - R_{a_{\min}}}, & R_{a_{\min}} \le R_{a_i} \le R_{a_{\max}} \\ 1, & R_a \le 0.21 \end{cases}$ |
| Desirability for tool life ($D_T$) (Eq. 27) | |
| $D_T = \begin{cases} 0, & T \le 6.7 \\ \dfrac{T_i - T_{\min}}{T_{\max} - T_{\min}}, & T_{\min} \le T_i \le T_{\max} \\ 1, & T \ge 40.3 \end{cases}$ | |

Table 10

**One-sided transformation for *MTCVD-TiCN/Al$_2$O$_3$* coated tools**

| Desirability for tangential cutting force ($DF_c$) (Eq. 28) | Desirability for feed force ($DF_f$) (Eq. 29) |
|---|---|
| $DF_c = \begin{cases} 0, & F_c \ge 220.4 \\ \dfrac{F_{c_{\max}} - F_{c_i}}{F_{c_{\max}} - F_{c_{\min}}}, & F_{c_{\min}} \le F_{c_i} \le F_{c_{\max}} \\ 1, & F_c \le 15.1 \end{cases}$ | $DF_f = \begin{cases} 0, & F_f \ge 78.3 \\ \dfrac{F_{f_{\max}} - F_{f_i}}{F_{f_{\max}} - F_{f_{\min}}}, & F_{f_{\min}} \le F_{f_i} \le F_{f_{\max}} \\ 1, & F_f \le 13.3 \end{cases}$ |
| Desirability for radial force ($DF_r$) (Eq. 30) | Desirability for surface roughness ($DR_a$) (Eq. 31) |
| $DF_r = \begin{cases} 0, & F_r \ge 34.6 \\ \dfrac{F_{r_{\max}} - F_{r_i}}{F_{r_{\max}} - F_{r_{\min}}}, & F_{r_{\min}} \le F_{r_i} \le F_{r_{\max}} \\ 1, & F_r \le 14 \end{cases}$ | $DR_a = \begin{cases} 0, & R_a \ge 1.59 \\ \dfrac{R_{a_{\max}} - R_{a_i}}{R_{a_{\max}} - R_{a_{\min}}}, & R_{a_{\min}} \le R_{a_i} \le R_{a_{\max}} \\ 1, & R_a \le 0.24 \end{cases}$ |
| Desirability for tool life ($D_T$) (Eq. 32) | |
| $D_T = \begin{cases} 0, & T \le 8.5 \\ \dfrac{T_i - T_{\min}}{T_{\max} - T_{\min}}, & T_{\min} \le T_i \le T_{\max} \\ 1, & T \ge 51.1 \end{cases}$ | |

Table 11

**Family of optimal solutions [*V* (m/min), *f* (mm/rev), *d* (mm)] for *PVD-AlTiN* coated (*C*) tools**

| Optimum parameters | Optimum responses | | | | | Desirability | | | | | Single desirability ($D_M$) |
|---|---|---|---|---|---|---|---|---|---|---|---|
| | $F_c$ (N) | $F_f$ (N) | $F_r$ (N) | $R_a$ (μm) | $T$ (min) | $DF_c$ | $DF_f$ | $DF_r$ | $DR_a$ | $D_T$ | |
| [200, 0.05, 0.1] | 28.15 | 10.82 | 8.96 | 0.38 | 37.70 | 0.97 | 0.97 | 0.92 | 0.86 | 1.00 | 0.94 |
| [210, 0.05, 0.1] | 27.88 | 10.65 | 8.87 | 0.36 | 36.16 | 0.97 | 0.97 | 0.92 | 0.87 | 0.95 | 0.94 |
| [220, 0.05, 0.1] | 27.63 | 10.49 | 8.79 | 0.35 | 34.76 | 0.97 | 0.97 | 0.93 | 0.89 | 0.91 | 0.93 |
| [230, 0.05, 0.1] | 27.39 | 10.34 | 8.72 | 0.33 | 33.46 | 0.97 | 0.97 | 0.93 | 0.90 | 0.87 | 0.93 |
| [240, 0.05, 0.1] | 27.17 | 10.20 | 8.65 | 0.32 | 32.27 | 0.98 | 0.98 | 0.94 | 0.91 | 0.83 | 0.92 |
| [250, 0.05, 0.1] | 26.95 | 10.07 | 8.58 | 0.31 | 31.17 | 0.98 | 0.98 | 0.94 | 0.92 | 0.79 | 0.92 |
| [260, 0.05, 0.1] | 26.75 | 9.94 | 8.52 | 0.30 | 30.14 | 0.98 | 0.98 | 0.95 | 0.92 | 0.76 | 0.91 |
| [270, 0.05, 0.1] | 26.55 | 9.83 | 8.46 | 0.29 | 29.19 | 0.98 | 0.98 | 0.95 | 0.93 | 0.73 | 0.91 |
| [280, 0.05, 0.1] | 26.36 | 9.71 | 8.40 | 0.28 | 28.29 | 0.98 | 0.98 | 0.96 | 0.94 | 0.70 | 0.91 |
| [290, 0.05, 0.1] | 26.18 | 9.60 | 8.34 | 0.27 | 27.46 | 0.98 | 0.98 | 0.96 | 0.95 | 0.68 | 0.90 |
| [200, 0.055, 0.1] | 29.32 | 11.80 | 9.18 | 0.40 | 35.54 | 0.95 | 0.95 | 0.90 | 0.85 | 0.93 | 0.92 |
| [210, 0.055, 0.1] | 29.04 | 11.62 | 9.10 | 0.38 | 34.09 | 0.96 | 0.95 | 0.90 | 0.86 | 0.89 | 0.91 |
| [220, 0.055, 0.1] | 28.78 | 11.45 | 9.02 | 0.36 | 32.77 | 0.96 | 0.96 | 0.91 | 0.87 | 0.85 | 0.91 |
| [230, 0.055, 0.1] | 28.53 | 11.28 | 8.94 | 0.35 | 31.55 | 0.96 | 0.96 | 0.92 | 0.88 | 0.81 | 0.90 |

Table 12

**Family of optimal solutions [*V* (m/min), *f* (mm/rev), *d* (mm)]**
**for *PVD-AlTiN* coated-microblasted (*CMB*) tools**

| Optimum parameters | Optimum responses | | | | | Desirability | | | | | Single desirability ($D_M$) |
|---|---|---|---|---|---|---|---|---|---|---|---|
| | $F_c$ (N) | $F_f$ (N) | $F_r$ (N) | $R_a$ (μm) | $T$ (min) | $DF_c$ | $DF_f$ | $DF_r$ | $DR_a$ | $D_T$ | |
| [200, 0.05, 0.1] | 17.60 | 14.70 | 8.71 | 0.39 | 40.36 | 0.97 | 0.95 | 0.96 | 0.86 | 1.00 | 0.95 |
| [210, 0.05, 0.1] | 17.12 | 14.47 | 8.64 | 0.37 | 38.90 | 0.97 | 0.95 | 0.96 | 0.87 | 0.96 | 0.94 |
| [220, 0.05, 0.1] | 16.68 | 14.25 | 8.57 | 0.36 | 37.56 | 0.98 | 0.96 | 0.96 | 0.89 | 0.92 | 0.94 |
| [230, 0.05, 0.1] | 16.27 | 14.04 | 8.51 | 0.34 | 36.32 | 0.98 | 0.96 | 0.97 | 0.90 | 0.88 | 0.94 |
| [240, 0.05, 0.1] | 15.89 | 13.84 | 8.45 | 0.33 | 35.17 | 0.98 | 0.96 | 0.97 | 0.91 | 0.85 | 0.93 |
| [250, 0.05, 0.1] | 15.53 | 13.65 | 8.39 | 0.32 | 34.10 | 0.98 | 0.97 | 0.97 | 0.91 | 0.81 | 0.93 |
| [260, 0.05, 0.1] | 15.19 | 13.47 | 8.33 | 0.31 | 33.11 | 0.98 | 0.97 | 0.97 | 0.92 | 0.78 | 0.92 |
| [270, 0.05, 0.1] | 14.88 | 13.31 | 8.28 | 0.30 | 32.18 | 0.99 | 0.97 | 0.98 | 0.93 | 0.76 | 0.92 |
| [200, 0.055, 0.1] | 19.03 | 15.85 | 9.35 | 0.41 | 37.94 | 0.96 | 0.93 | 0.93 | 0.84 | 0.93 | 0.92 |
| [280, 0.05, 0.1] | 14.58 | 13.15 | 8.23 | 0.29 | 31.31 | 0.99 | 0.97 | 0.98 | 0.94 | 0.73 | 0.92 |
| [210, 0.055, 0.1] | 18.52 | 15.59 | 9.27 | 0.39 | 36.57 | 0.97 | 0.93 | 0.93 | 0.86 | 0.89 | 0.91 |
| [200, 0.055, 0.12] | 21.04 | 15.91 | 9.16 | 0.42 | 37.88 | 0.95 | 0.93 | 0.94 | 0.83 | 0.93 | 0.91 |
| [290, 0.05, 0.1] | 14.30 | 12.99 | 8.18 | 0.28 | 30.49 | 0.99 | 0.98 | 0.98 | 0.95 | 0.71 | 0.91 |
| [210, 0.05, 0.12] | 20.47 | 15.65 | 9.08 | 0.40 | 36.51 | 0.96 | 0.93 | 0.94 | 0.85 | 0.89 | 0.91 |
| [220, 0.055, 0.1] | 18.04 | 15.35 | 9.20 | 0.38 | 35.31 | 0.97 | 0.94 | 0.94 | 0.87 | 0.85 | 0.91 |
| [300, 0.05, 0.1] | 14.03 | 12.85 | 8.13 | 0.27 | 29.72 | 0.99 | 0.98 | 0.98 | 0.95 | 0.68 | 0.91 |
| [220, 0.05, 0.12] | 19.95 | 15.41 | 9.01 | 0.39 | 35.25 | 0.96 | 0.94 | 0.94 | 0.86 | 0.85 | 0.91 |

The End Table 12

| Optimum parameters | Optimum responses | | | | | Desirability | | | | | Single desirability ($D_M$) |
|---|---|---|---|---|---|---|---|---|---|---|---|
| | $F_c$ (N) | $F_f$ (N) | $F_r$ (N) | $R_a$ (μm) | $T$ (min) | $DF_c$ | $DF_f$ | $DF_r$ | $DR_a$ | $D_T$ | |
| [230, 0.055, 0.1] | 17.60 | 15.13 | 9.13 | 0.36 | 34.15 | 0.97 | 0.94 | 0.94 | 0.88 | 0.82 | 0.91 |
| [310, 0.05, 0.1] | 13.77 | 12.71 | 8.09 | 0.27 | 28.99 | 0.99 | 0.98 | 0.98 | 0.96 | 0.66 | 0.91 |
| [230, 0.05, 0.12] | 19.46 | 15.19 | 8.94 | 0.37 | 34.08 | 0.96 | 0.94 | 0.95 | 0.87 | 0.81 | 0.90 |
| [240, 0.055, 0.1] | 17.18 | 14.92 | 9.06 | 0.35 | 33.07 | 0.97 | 0.94 | 0.94 | 0.89 | 0.78 | 0.90 |
| [320, 0.05, 0.1] | 13.53 | 12.57 | 8.04 | 0.26 | 28.31 | 0.99 | 0.98 | 0.99 | 0.96 | 0.64 | 0.90 |
| [240, 0.05, 0.12] | 19.00 | 14.97 | 8.88 | 0.36 | 33.01 | 0.96 | 0.94 | 0.95 | 0.88 | 0.78 | 0.90 |
| [250, 0.055, 0.1] | 16.80 | 14.71 | 9.00 | 0.34 | 32.06 | 0.98 | 0.95 | 0.94 | 0.90 | 0.75 | 0.90 |

Table 13

**Family of optimal solutions [*V* (m/min), *f* (mm/rev), *d* (mm)] for *MTCVD-TiCN/$Al_2O_3$* coated tools**

| Optimum parameters | Optimum responses | | | | | Desirability | | | | | Single desirability ($D_M$) |
|---|---|---|---|---|---|---|---|---|---|---|---|
| | $F_c$ (N) | $F_f$ (N) | $F_r$ (N) | $R_a$ (μm) | $T$ (min) | $DF_c$ | $DF_f$ | $DF_r$ | $DR_a$ | $D_T$ | |
| [200, 0.05, 0.1] | 21.20 | 14.23 | 15.48 | 0.37 | 51.14 | 0.97 | 0.99 | 0.93 | 0.91 | 1.00 | 0.96 |
| [210, 0.05, 0.1] | 20.70 | 14.17 | 15.37 | 0.36 | 48.90 | 0.97 | 0.99 | 0.93 | 0.92 | 0.95 | 0.95 |
| [220, 0.05, 0.1] | 20.24 | 14.11 | 15.27 | 0.35 | 46.86 | 0.98 | 0.99 | 0.94 | 0.92 | 0.90 | 0.94 |
| [230, 0.05, 0.1] | 19.81 | 14.05 | 15.17 | 0.34 | 44.98 | 0.98 | 0.99 | 0.94 | 0.93 | 0.86 | 0.94 |
| [240, 0.05, 0.1] | 19.40 | 13.99 | 15.08 | 0.33 | 43.26 | 0.98 | 0.99 | 0.95 | 0.94 | 0.82 | 0.93 |
| [200, 0.05, 0.12] | 24.61 | 15.49 | 15.70 | 0.41 | 48.20 | 0.95 | 0.97 | 0.92 | 0.88 | 0.93 | 0.93 |
| [200, 0.055, 0.1] | 23.17 | 15.47 | 16.42 | 0.39 | 48.39 | 0.96 | 0.97 | 0.88 | 0.89 | 0.94 | 0.93 |
| [250, 0.05, 0.1] | 19.02 | 13.94 | 14.99 | 0.32 | 41.67 | 0.98 | 0.99 | 0.95 | 0.94 | 0.78 | 0.93 |
| [210, 0.05, 0.12] | 24.03 | 15.42 | 15.59 | 0.40 | 46.09 | 0.96 | 0.97 | 0.92 | 0.89 | 0.88 | 0.92 |
| [210, 0.055, 0.1] | 22.62 | 15.40 | 16.30 | 0.38 | 46.27 | 0.96 | 0.97 | 0.89 | 0.90 | 0.89 | 0.92 |
| [260, 0.05, 0.1] | 18.66 | 13.89 | 14.91 | 0.32 | 40.20 | 0.98 | 0.99 | 0.96 | 0.95 | 0.74 | 0.92 |
| [220, 0.05, 0.12] | 23.50 | 15.35 | 15.49 | 0.39 | 44.17 | 0.96 | 0.97 | 0.93 | 0.90 | 0.84 | 0.92 |
| [220, 0.055, 0.1] | 22.12 | 15.33 | 16.20 | 0.37 | 44.34 | 0.97 | 0.97 | 0.89 | 0.91 | 0.84 | 0.91 |
| [270, 0.05, 0.1] | 18.33 | 13.84 | 14.83 | 0.31 | 38.83 | 0.98 | 0.99 | 0.96 | 0.95 | 0.71 | 0.91 |
| [230, 0.05, 0.12] | 23.00 | 15.29 | 15.39 | 0.38 | 42.40 | 0.96 | 0.97 | 0.93 | 0.90 | 0.80 | 0.91 |
| [230, 0.055, 0.1] | 21.65 | 15.27 | 16.09 | 0.36 | 42.57 | 0.97 | 0.97 | 0.90 | 0.92 | 0.80 | 0.91 |
| [280, 0.05, 0.1] | 18.00 | 13.79 | 14.76 | 0.30 | 37.56 | 0.99 | 0.99 | 0.96 | 0.96 | 0.68 | 0.91 |
| [240, 0.05, 0.12] | 22.53 | 15.23 | 15.30 | 0.37 | 40.78 | 0.96 | 0.97 | 0.94 | 0.91 | 0.76 | 0.90 |
| [200, 0.05, 0.14] | 27.92 | 16.63 | 15.89 | 0.44 | 45.85 | 0.94 | 0.95 | 0.91 | 0.85 | 0.88 | 0.90 |
| [240, 0.055, 0.1] | 21.20 | 15.21 | 16.00 | 0.35 | 40.94 | 0.97 | 0.97 | 0.90 | 0.92 | 0.76 | 0.90 |
| [290, 0.05, 0.1] | 17.70 | 13.75 | 14.68 | 0.30 | 36.37 | 0.99 | 0.99 | 0.97 | 0.96 | 0.65 | 0.90 |

Validatory experiments are conducted under optimal cutting conditions for the different tools considered in the present study. Table 14 depicts that the predicted results of cutting forces at optimal cutting conditions for different tools using developed mathematical models are in good agreement with the experimental results. The error in the predicted and experimental results is less than 15 % for cutting forces and less than

10 % for surface roughness and tool life. It demonstrates that, within the range of the chosen parameters and using different tools taken into account in the current study, the developed model could be used to accurately predict *AISI 304* turning responses.

Table 14

**Validatory experimental matrix at optimum parameters**
**[*V* (m/min), *f* (mm/rev), *d* (mm)]**

| Optimum parameters | Tool type | Model results (Eq. 11–13) | | | | | Experimental results | | | | |
|---|---|---|---|---|---|---|---|---|---|---|---|
| | | $F_c$ (N) | $F_f$ (N) | $F_r$ (N) | $R_a$ (µm) | $T$ (min) | $F_c$ (N) | $F_f$ (N) | $F_r$ (N) | $R_a$ (µm) | $T$ (min) |
| [230, 0.055, 0.1] | *C* | 28.53 | 11.28 | 8.94 | 0.35 | 31.55 | 29 | 11 | 11 | 0.39 | 34 |
| [200, 0.05, 0.1] | *C* | 28.15 | 10.82 | 8.96 | 0.38 | 37.70 | 33 | 14 | 10 | 0.33 | 36 |
| [250, 0.055, 0.1] | *CMB* | 16.80 | 14.71 | 9.00 | 0.34 | 32.06 | 21 | 18 | 11 | 0.29 | 27 |
| [200, 0.15, 0.2] | *CMB* | 17.60 | 14.70 | 8.71 | 0.39 | 40.36 | 21 | 17 | 12 | 0.36 | 36 |
| [290, 0.05, 0.1] | *MTCVD* | 17.70 | 13.75 | 14.68 | 0.30 | 36.37 | 23 | 16 | 16 | 0.33 | 33 |
| [200, 0.05, 0.1] | *MTCVD* | 21.20 | 14.23 | 15.48 | 0.37 | 51.14 | 24 | 19 | 17 | 0.39 | 47 |

This study strongly recommends *MTCVD-TiCN/*$Al_2O_3$ coated tools for finishing turning of *AISI 304* stainless steel using $V$ = 200–290 m/min and lower values of $f$ and $d$. This study did not consider the tool wear effect on cutting forces and finds scope to model forces considering the tool wear effect in the turning of *AISI 304* with differently pre-and post-treated coated tools.

## Conclusions

In the current study, the dry turning performance of *AISI 304* stainless steel with single-layer *PVD-AlTiN* coated, single-layer *PVD-AlTiN* coated and microblasted, and *MTCVD-TiCN/*$Al_2O_3$ coated (*MTCVD*) tools is evaluated. The following conclusions can be drawn from the present study.

1. *PVD-AlTiN* coated tools provide the lowest cutting forces and surface roughness, followed by *PVD-AlTiN* coated-microblasted and *MTCVD-TiCN/*$Al_2O_3$ coated tools. However, these responses were marginally differed for coated and coated-microblasted tools.

2. The cutting forces decrease with the cutting parameters. However, this effect is significant for *MTCVD-TiCN/*$Al_2O_3$ coated tools. On the other hand, higher tool life is observed for *MTCVD-TiCN/*$Al_2O_3$ coated tools, followed by *PVD-AlTiN* coated-microblasted and *PVD-AlTiN* coated tools.

3. The correlation coefficients observed above 0.9 for the developed models showed that the developed models can be used reliably to predict the responses studied during turning *AISI 304* within the range of the parameters considered in this study.

4. The optimization study reveals that turning of *AISI 304* with *MTCVD-TiCN/*$Al_2O_3$ coated tools incurs lower cutting forces of 18–27 N, produces a minimum surface roughness of 0.3–0.44 µm, and has a better tool life of 36–51 min compared to *PVD-AlTiN* coated (*C*) and *PVD-AlTiN* coated-microblasted (*CMB*) tools.

5. This study strongly recommends *MTCVD-TiCN/*$Al_2O_3$ coated tools for finishing turning of *AISI 304* stainless steel using $V$ = 200–290 m/min and lower values of $f$ and $d$.

## References

1. He H.B., Li H.Y., Yang J., Zhang X.Y., Yue Q.B., Jiang X., Lyu S.K. A study on major factors influencing dry cutting temperature of AISI 304 stainless steel. *International Journal of Precision Engineering and Manufacturing*, 2017, vol. 18, pp. 1387–1392. DOI: 10.1007/s12541-017-0165-6.

2. Rao V.D.P., Ali S.R.M., Ali S.M.S., Geethika V.N. Multi-objective optimization of cutting parameters in CNC turning of stainless steel 304 with TiAlN nano coated tool. *Materials Today: Proceedings*, 2018, vol. 5 (12), pp. 25789–25797. DOI: 10.1016/j.matpr.2018.06.571.

3. Kulkarni A., Sargade V., More C. Machinability investigation of AISI 304 austenitic stainless steels using multilayer AlTiN/TiAlN coated carbide inserts. *Procedia Manufacturing*, 2018, vol. 20, pp. 548–553. DOI: 10.1016/j.promfg.2018.02.082.

4. Bouzid L., Berkani S., Yallese M., Girardin F., Mabrouki T. Estimation and optimization of flank wear and tool lifespan in finish turning of AISI 304 stainless steel using desirability function approach. *International Journal of Industrial Engineering Computations*, 2018, vol. 9 (3), pp. 349–368. DOI: 10.5267/j.ijiec.2017.8.002.

5. Sharma N., Gupta K. Influence of coated and uncoated carbide tools on tool wear and surface quality during dry machining of stainless steel 304. *Materials Research Express*, 2019, vol. 6 (8), p. 086585. DOI: 10.1088/2053-1591/ab1e59.

6. Patel U.S., Rawal S.K., Arif A.F.M., Veldhuis S.C. Influence of secondary carbides on microstructure, wear mechanism, and tool performance for different cermet grades during high-speed dry finish turning of AISI 304 stainless steel. *Wear*, 2020, vol. 452, p. 203285. DOI: 10.1016/j.wear.2020.203285.

7. Dubovska R., Majerik J., Chochlikova H. Investigation of durability $T = f(v_c)$ in turning of the AISI 304 austenitic stainless steel using the CNMG 120408 coated carbide insert. *Advanced Materials Research*, 2014, vol. 941, pp. 1633–1643. DOI: 10.4028/www.scientific.net/AMR.941-944.1633.

8. Sharma A.K., Tiwari A.K., Dixit A.R., Singh R.K. Measurement of machining forces and surface roughness in turning of AISI 304 steel using alumina-MWCNT hybrid nanoparticles enriched cutting fluid. *Measurement*, 2020, vol. 150, p. 107078. DOI: 10.1016/j.measurement.2019.107078.

9. Rao V.D.P., Harsha N., Ram N.R., Geethika V.N. Optimization of cutting parameters in CNC turning of stainless steel 304 with TiAlN nano coated carbide cutting tool. *IOP Conference Series: Materials Science and Engineering*, 2018, vol. 310 (1), p. 012109. DOI: 10.1088/1757-899X/310/1/012109.

10. Chen K.T., Hu C.C., Hsu C.Y., Tsao C.C., Hong P.D. Optimizing the multiattribute characteristics of CrWN hard film tool in turning AISI 304 stainless steel. *Journal of Materials Engineering and Performance*, 2020, vol. 29, pp. 2506–2513. DOI: 10.1007/s11665-020-04732-x.

11. Patil N., Gopalakrishna K., Sangmesh B., Sudhakar K., Vijaykumar G.C. Performance studies on cryogenic treated carbide cutting tool for turning of AISI304 steel. *Journal of Mechanical Engineering and Sciences*, 2018, vol. 12 (3), pp. 3927–3941. DOI: 10.15282/jmes.12.3.2018.12.0343.

12. Singh T., Dureja J.S., Dogra M., Bhatti M.S. Multi-response optimization in environment friendly turning of AISI 304 austenitic stainless steel. *Multidiscipline Modeling in Materials and Structures*, 2019, vol. 15 (3), pp. 538–558. DOI: 10.1108/MMMS-07-2018-0139.

13. Lubis S., Rosehan, Darmawan S., Adianto, Malik R. The influence of cutting speed variation in turning of AISI 304 materials on wear and tool life coated carbide cutting tools. *International Journal of Mechanical Engineering and Technology*, 2019, vol. 10 (6), pp. 203–210.

14. Khan S.A., Shamail S., Anwar S., Hussain A., Ahmad S., Saleh M. Wear performance of surface treated drills in high-speed drilling of AISI 304 stainless steel. *Journal of Manufacturing Processes*, 2020, vol. 58, pp. 223–235. DOI: 10.1016/j.jmapro.2020.08.022.

15. Bedi S.S., Behera G.C., Datta S. Effects of cutting speed on MQL machining performance of AISI 304 stainless steel using uncoated carbide insert: application potential of coconut oil and rice bran oil as cutting fluids. *Arabian Journal for Science and Engineering*, 2020, vol. 45, pp. 8877–8893. DOI: 10.1007/s13369-020-04554-y.

16. Rathod N.J., Chopra M.K., Chaurasiya P.K., Vidhate U.S., Dasore A. Optimization on the turning process parameters of SS 304 using Taguchi and TOPSIS. *Annals of Data Science*, 2023, vol. 10, pp. 1405–1419. DOI: 10.1007/s40745-021-00369-2.

17. Sivaiah P., Revantha Kumar M., Bala Subramanyam S., Prasad K.L.V. A comparative study on different textured and untextured tools performance in turning process. *Materials and Manufacturing Processes*, 2021, vol. 36 (8), pp. 926–935. DOI: 10.1080/10426914.2020.1866201.

18. Moganapriya C., Rajasekar R., Santhosh R., Saran S., Santhosh S., Gobinath V.K., Kumar P.S. Sustainable hard machining of AISI 304 stainless steel through TiAlN, AlTiN, and TiAlSiN coating and multi-criteria decision making using grey fuzzy coupled Taguchi method. *Journal of Materials Engineering and Performance*, 2022, vol. 31 (9), pp. 7302–7314. DOI: 10.1007/s11665-022-06751-2.

19. Bedi S.S., Sahoo S.P., Vikas B., Datta S. Influence of cutting speed on dry machinability of AISI 304 stainless steel. *Materials Today: Proceedings*, 2021, vol. 38, pp. 2174–2180. DOI: 10.1016/j.matpr.2020.05.554.

20. Kulkarni A., Ambhore N., Deshpande A., Anerao P., Chinchanikar S. Analysis of cutting temperature during turning of SS 304 using uncoated and PVD coated carbide inserts. *Materials Today: Proceedings*, 2022, vol. 68, pp. 2569–2573. DOI: 10.1016/j.matpr.2022.09.417.

21. Patel U., Rawal S., Bose B., Arif A.F.M., Veldhuis S. Performance evaluations of Ti-based PVD coatings deposited on cermet tools for high-speed dry finish turning of AISI 304 stainless steel. *Wear*, 2022, vol. 492, p. 204214. DOI: 10.1016/j.wear.2021.204214.

22. Özbek N.A., Karadag M.İ., Özbek O. Optimization of flank wear and surface roughness during turning of AISI 304 stainless steel using the Taguchi method. *Materials Testing*, 2020, vol. 62 (9), pp. 957–961. DOI: 10.3139/120.111571.

23. Gaikwad V.S., Chinchanikar S. Mechanical behaviour of friction stir welded AA7075-T651 joints considering the effect of tool geometry and process parameters. *Advances in Materials and Processing Technologies*, 2022, vol. 8 (4), pp. 3730–3748. DOI: 10.1080/2374068X.2021.1976554.

24. Chinchanikar S., Choudhury S.K. Effect of work material hardness and cutting parameters on performance of coated carbide tool when turning hardened steel: An optimization approach. *Measurement*, 2013, vol. 46 (4), pp. 1572–1584. DOI: 10.1016/j.measurement.2012.11.032.

## Conflicts of Interest

The authors declare no conflict of interest.